IOP PUBLISHING PHYSIOLOGICAL MEASUREMENT

Physiol. Meas. **33** (2012) 1975–1991 doi:10.1088/0967-3334/33/12/1975

Characterization of ventricular depolarization and repolarization changes in a porcine model of myocardial infarction

Daniel Romero[1,2], Michael Ringborn[3,4], Marina Demidova[3,5], Sasha Koul[3], Pablo Laguna[1,2], Pyotr G Platonov[3] and Esther Pueyo[1,2]

[1] Aragón Institute of Engineering Research—I3A, University of Zaragoza, Mariano Esquillor, s/n, 50018, Zaragoza, Spain
[2] CIBER de Bioingeniería, Biomateriales y Nanomedicina, Zaragoza, Spain
[3] Department of Cardiology, Clinical Sciences, Lund University, Lund, Sweden
[4] Thoracic Center, Blekingesjukhuset Karlskrona, Sweden
[5] Federal Center of Heart, Blood and Endocrinology, St Petersburg, Russia

E-mail: daromero@unizar.es

Received 18 August 2012, accepted for publication 12 October 2012
Published 9 November 2012
Online at stacks.iop.org/PM/33/1975

Abstract

In this study, several electrocardiogram (ECG)-derived indices corresponding to both ventricular depolarization and repolarization were evaluated during acute myocardial ischemia in an experimental model of myocardial infarction produced by 40 min coronary balloon inflation in 13 pigs. Significant changes were rapidly observed from minute 4 after the start of coronary occlusion, achieving their maximum values between 11 and 22 min for depolarization and between 9 and 12 min for repolarization indices, respectively. Subsequently, these maximum changes started to decrease during the latter part of the occlusion. Depolarization changes associated with the second half of the QRS complex showed a significant but inverse correlation with the myocardium at risk (MaR) estimated by scintigraphic images. The correlation between MaR and changes of the downward slope of the QRS complex, $\mathcal{I}_{\mathrm{DS}}$, evaluated at the two more relevant peaks observed during the occlusion, was $r = -0.75$, $p < 0.01$ and $r = -0.79$, $p < 0.01$ for the positive and negative deflections observed in $\mathcal{I}_{\mathrm{DS}}$ temporal evolution, respectively. Repolarization changes, analyzed by evaluation of ST segment elevation at the main observed positive peak, also showed negative, however non-significant correlation with MaR: $r = -0.34$, $p = 0.28$. Our results suggest that changes evaluated in the latter part of the depolarization, such as those described by $\mathcal{I}_{\mathrm{DS}}$, which are influenced by R-wave amplitude, QRS width and ST level variations simultaneously,

correlate better with the amount of ischemia than other indices evaluated in the earlier part of depolarization or during the ST segment.

Keywords: ischemia, PCI, depolarization, QRS slopes

1. Introduction

Treatment of acute myocardial infarction has improved significantly during the last few years due to early reperfusion strategies with primary percutaneous coronary intervention (PCI) as well as more efficient pharmaceutical approaches, especially antiplatelet drugs. Early, acute decision making, often already in the pre-hospital phase, is based on the standard 12-lead electrocardiogram (ECG), which can be transmitted digitally to the attending cardiologist or emergency physician. Depending on whether ST-elevation myocardial infarction (STEMI) criteria are met or not, the patient then is transferred either to a regional PCI center or to the local hospital for further treatment.

The STEMI criteria are based solely upon changes in the repolarization phase of the ECG. However, severe myocardial ischemia due to lack of ischemia protection in the myocardium (such as collaterals and/or metabolic preconditioning) causes slowing of the conduction through the ischemic myocardium, thus producing changes also in the depolarization phase (QRS complex). Since longer time is needed for the activation wavefront to propagate through the ischemic area, the normal, balanced ventricular depolarization is altered, thus producing changes in the QRS complex. The more severe ischemia makes the progression of irreversible necrosis due to evolving myocardial infarction faster over time compared to a situation when the myocardium is more protected. By also considering changes in the depolarization phase in the early triage of patients, important risk stratification can be made, adding prognostic information as well as enabling tailoring of the acute management.

Earlier studies on depolarization changes during ischemia due to acute coronary occlusion both in humans and animals have considered QRS prolongation (Weston *et al* 2007), amplitude changes of the R and S waves (Charlap *et al* 1990), 'distortion' of the terminal part of the QRS complex (Birnbaum *et al* 1996) and changes in the high-frequency components of the QRS complex (Pettersson *et al* 2000, Abboud *et al* 1987, Beker *et al* 1996). However, these results have not yet been implemented in clinical practice. More studies are needed to understand the pathophysiological bases of these QRS changes, but also to develop robust and validated methods to correctly characterize and quantify them. We have proposed a method for evaluation of depolarization changes by analyzing the slopes of the QRS complex: upward slope between Q and R waves ($\mathcal{I}_{\mathrm{US}}$) and downward slope between R and S waves ($\mathcal{I}_{\mathrm{DS}}$) (Romero *et al* 2011). Since simultaneous ST elevation obscures the delineation between the end of the depolarization and beginning of the repolarization, QRS prolongation during ischemia is difficult to correctly determine, which is why the QRS slope method offers a more robust way taking into consideration the overall change in the depolarization phase including both duration and amplitude changes. During coronary artery occlusion by PCI in humans, the QRS slopes became considerably less steep than in the control situation, in particular for $\mathcal{I}_{\mathrm{DS}}$, as a combined result of both changes of the QRS amplitude and duration. The method has shown very low intra-individual variation in a control situation, and both changes in $\mathcal{I}_{\mathrm{US}}$ and $\mathcal{I}_{\mathrm{DS}}$ during the ischemia have proven to correlate significantly with the amount of ischemia as determined by myocardial scintigraphy (Ringborn *et al* 2011).

A number of animal experiments have been carried out to investigate whether changes in the ECG, mostly in the ST-T interval, are related to the amount of ischemia assessed either by different image techniques or by histochemical analysis. In pigs, during regional ischemia produced by clamping one of the coronary arteries (mainly the left anterior descending (LAD) artery), changes were reflected as T-Q depression, decreased action potential amplitude and upstroke velocity (Chang *et al* 1989, Janse *et al* 1979, Morena *et al* 1980). Also, changes in QRS vector (magnitude and direction) (Näslund *et al* 1993a), and ST vector (Näslund *et al* 1993b) have been reported, and were also correlated with the myocardium at risk (MaR) during the initial minutes of ischemia.

In this study we further evaluated the slope indices of the ventricular depolarization phase by expanding our model from short-term ischemia in humans (Romero *et al* 2011, Ringborn *et al* 2011) to an experimental porcine model of myocardial infarction. The specific aims of this study were to:

(i) Characterize the dynamics of different depolarization and repolarization indices during balloon-induced ischemia in pigs in the 12 standard ECG leads, normalized leads and QRS loop-derived leads.
(ii) Correlate changes of these indices to the amount of ischemia given by MaR determined by myocardial perfusion imaging (MPS).

2. Materials and methods

2.1. Study population

The study population comprised 13 domestic pigs with a weight range between 40–50 kg. During anesthesia, ischemia was induced by 40 min long occlusion of the LAD artery achieved by inflation of a percutaneous transluminal balloon placed in the middle part of the vessel. MPS was used to evaluate the amount of MaR (Heiberg *et al* 2010). A detailed description of experimental setup is given elsewhere (Demidova *et al* 2011).

2.1.1. ECG recording. During the occlusion procedure, a continuous standard 12-lead ECG recording was acquired using a digital ECG monitor ('Kardiotechnica-04-8m', Incart, St Petersburg, Russia) with a sampling rate of 1024 Hz and amplitude resolution of 40 μV per LSB (least significant bit). In addition, both a baseline ECG recording before occlusion as well as a 4 h reperfusion recording after the 40 min occlusion were acquired, thus achieving a total experiment protocol duration of 5 h. The hearts were then explanted for later *ex-vivo* imaging acquisition. In this study only the 40 min corresponding to the occlusion period were considered for analysis.

2.1.2. Image acquisition and processing for assessment of MaR. Approximately 1000 MBq of Tetrofosmin Tc-99m was injected intravenously into each pig at 20 min of LAD occlusion. The MPS *ex-vivo* imaging was carried out by a dual-head camera (Skylight, Philips, Best, The Netherlands) at 32 projections (40 s per projection) with 64 $\times$ 64 matrix yielding a digital resolution of 5 $\times$ 5 $\times$ 5 mm^3. A low resolution Butterworth filter with a cutoff frequency of 0.6 of Nyquist rate (half sampling rate) and order 5 was applied for iterative reconstruction using maximum likelihood-expectation maximization. Short- and long-axis images were reconstructed (Demidova *et al* 2011). To analyze the MPS images and assess the MaR the freely available software Segment v1.700 (Medviso, Lund, Sweden; http://segment.heiberg.se) was used (Heiberg *et al* 2010). The MaR was defined as the perfusion defect size, determined

by the area within the left ventricular (LV) myocardium with counts lower than 55% of the maximum (normal) counts, and expressed as a percentage of the total LV myocardium.

2.2. Preprocessing of the ECG signal

All the ECG recordings used in the study were preprocessed before computing the depolarization and repolarization indices. First, the QRS complexes were automatically detected (Martínez *et al* 2004) and then visually checked using the BiosigBrowser tool (Bolea *et al* 2009). This software was also used to manually classify the abnormal beats (ectopic, supraventricular, etc) from the automatic QRS complex detection, and discard them from further processing. Subsequent steps were: baseline drift attenuation via cubic spline interpolation and delineation using a wavelet-based technique (Martínez *et al* 2004). Only leads V1 to V6 were considered for the analysis.

2.3. Depolarization indices and lead configurations applied

2.3.1. QRS slopes and R-wave amplitude. For each pig the following depolarization indices were evaluated in the standard leads V1–V6:

- $\mathcal{I}_{\mathrm{US}}$: the upward slope of the R wave.
- $\mathcal{I}_{\mathrm{DS}}$: the downward slope of the R wave.
- R_a: R-wave amplitude.

The full methodology used to compute the QRS slope indices $\mathcal{I}_{\mathrm{US}}$ and $\mathcal{I}_{\mathrm{DS}}$ is described in detail in Romero *et al* (2011) and Pueyo *et al* (2008). R-wave amplitude R_a was measured using the PQ segment in each beat as the isoelectrical level.

$\mathcal{I}_{\mathrm{US}}$ and $\mathcal{I}_{\mathrm{DS}}$ were also evaluated in another lead derived from the spatial QRS loop using the vectorcardiogram (VCG). That alternative lead was obtained by projecting the VCG onto the direction associated with the maximum vector magnitude within the loop (Romero *et al* 2011). The orthogonal leads X, Y and Z used to compute the VCG were obtained by applying the Dower inverse matrix (DIM) (Edenbrandt and Pahlm 1988).

In addition to the standard and loop-derived leads, normalized ECG leads were generated. In brief, the maximum vector magnitude within the spatial QRS loop was used as a normalization factor for each corresponding beat. This maximum vector magnitude is denoted by $\mathrm{QRS}_{\mathrm{max}_i}$, where i represents the beat index used to normalize each ith beat in each lead l (V1–V6), $b_{i,l}(n)$, and the normalized beat $\hat{b}_{i,l}(n)$ is computed as:

$$\hat{b}_{i,l}(n) = \frac{b_{i,l}(n)}{\mathrm{QRS}_{\mathrm{max}_i}}. \tag{1}$$

The six normalized leads, obtained from precordial leads V1–V6 and denoted by nV1–nV6, were used to evaluate the $\mathcal{I}_{\mathrm{US}}$ and $\mathcal{I}_{\mathrm{DS}}$ indices as a way to investigate the relevance of slope changes generated just by QRS width changes, avoiding R wave amplitude influence. In this way it is possible to ascertain whether the slope-relevant information comes mostly from variations in QRS width or amplitude.

2.3.2. VCG-derived $\mathrm{QRS}_{\mathrm{max}}$ *and* $\mathrm{QRS}_{\mathrm{mean}}$. Other indices reported in the literature derived from the VCG were also evaluated in this study:

- $\mathrm{QRS}_{\mathrm{max}}$: maximum spatial QRS vector magnitude.
- $\mathrm{QRS}_{\mathrm{mean}}$: mean spatial QRS vector magnitude.

Table 1. (A) Summary of the ECG indices of the depolarization and repolarization phases and in which leads they were calculated. (B) Different ways the dynamic changes of the parameters were expressed (either as a single-lead maximum value or as a summation among leads), and later used for correlation analyses.

(A) Index ($\mathcal{Y}$)	Description	Lead configurations applied
$\mathcal{I}_{US}$	Upward slope of the R wave	V1–V6, nV1–nV6 and LDL (loop-derived lead)
$\mathcal{I}_{DS}$	Downward slope of the R wave	V1–V6, nV1–nV6 and LDL
R_a	R-wave amplitude	V1–V6
ST_{40}	ST level at $J + 40$ ms	V1–V6
QRS_{max}	Maximum QRS vector magnitude	VCG (vectorcardiogram)
QRS_{mean}	Mean QRS vector magnitude	VCG
STVM	ST vector magnitude	VCG
STCVM	ST change vector magnitude	VCG

(B) Different combinations of changes

$\Delta\mathcal{Y}_{max}$ (*): maximum change regardless lead (applied to both positive and negative deflections)
$\Delta\mathcal{Y}_{pos/neg}$ (*): sum of the positive (or negative) changes among leads evaluated at t_{max}
$\Delta\mathcal{Y}_{abs}$ (*): sum of absolute changes for all leads evaluated at t_{max}
$\Delta\mathcal{Y}_{real}$ (*): sum of all changes over leads keeping their original sign
$\Delta\mathcal{Y}^l_{max}$, $l = 1, \ldots, 6$ (leads V1–V6) or another transformed lead (LDL or from VCG)
t^l_{max}, $l = 1, \ldots, 6$ (leads V1–V6) or another transformed lead (LDL or from VCG)

(*) Only evaluated for $\mathcal{I}_{US}$, $\mathcal{I}_{DS}$, R_a and ST_{40} measured in standard leads V1–V6.

Details on how to compute both indices can be found in Näslund *et al* (1993a). Note that QRS_{max} represents the same normalization factor used in the previous section.

All depolarization indices described above, evaluated either in original, normalized and loop derived leads or derived from VCG, are summarized in table 1.

2.4. Repolarization indices

Conventional ST level deviation was determined in the precordial standard leads V1–V6. The ST level was measured 40 ms after the J point, with the PQ segment used as the isolectrical level, and denoted by ST_{40}. Two additional indices related to the ST segment were also calculated using the orthogonal leads X, Y and Z as described in Näslund *et al* (1993b):

- STVM: ST vector magnitude
- STCVM: ST change vector magnitude

The first index represents the spatial ST vector magnitude (STVM), calculated from J point + 20 ms. The second index represents the spatial ST change vector magnitude, determined by the magnitude of the vector difference between a reference (calculated in the first 5 s of the occlusion) and the current ST vector, both evaluated at $J + 20$ ms. ST_{40}, STVM and STCVM indices, as well as the other indices described in 2.3, were evaluated on a beat-to-beat basis during the whole occlusion procedure. The repolarization indices evaluated are also listed in table 1.

2.5. Quantification of ECG changes

The absolute change during the coronary occlusion was calculated for each analyzed index $\mathcal{Y}$ ($\mathcal{Y} \in \{\mathcal{I}_{US}, \mathcal{I}_{DS}, R_a, ST_{40}, QRS_{max}, QRS_{mean}, STVM, STCVM\}$) in each lead l ($l = 1, \ldots, 6$ for leads V1, ..., V6) by the parameter $\Delta\mathcal{Y}(t)$. This parameter was computed every 10 s from the beginning of the occlusion ($t = 0$) until the end ($t = 40$ min) in each lead l, and was defined

as the difference between the index value at time instant t, $\mathcal{Y}(t)$, and the reference value $\mathcal{Y}_{\text{ref}}$ given by the mean of $\mathcal{Y}$ in the first 5 s of occlusion, $\Delta\mathcal{Y}(t) = \mathcal{Y}(t) - \mathcal{Y}_{\text{ref}}$.

Delta changes $\Delta\mathcal{Y}(t)$ during the occlusion were averaged over pigs for each index $\mathcal{Y}$ to assess global behavior. Values for maximum delta change $\Delta\mathcal{Y}^l_{\text{max}}$ for each index were determined in each lead l for the relevant peaks along the occlusion period. Their corresponding timings t^l_{max} were identified, in both individual subjects and as mean for the whole population.

Different combinations of change were defined and were correlated with MaR. All these combinations are listed in table 1. The timing associated with $\Delta\mathcal{Y}_{\text{max}}$ was denoted by t_{max}. $\Delta\mathcal{Y}_{\text{pos/neg}}$,$\Delta\mathcal{Y}_{\text{abs}}$ and $\Delta\mathcal{Y}_{\text{real}}$ were computed based on this specific timing (t_{max}). For $\Delta\mathcal{Y}_{\text{max}}$ and $\Delta\mathcal{Y}_{\text{pos/neg}}$ there are two possibilities of calculation depending on whether the peak observed in the index corresponds to a positive or a negative value. $\Delta\mathcal{Y}^l_{\text{max}}$ and t^l_{max} values were correlated with MaR both individually and in combination, separately for each lead l. The definitions of $\Delta\mathcal{Y}^l_{\text{max}}$ and its corresponding timing t^l_{max} are analogous to those of $\Delta\mathcal{Y}_{\text{max}}$ and t_{max}, but just for an individual lead l.

2.6. Statistical methods

Results are presented as mean ± standard deviation (SD). Because of the small number of subjects in the study, nonparametric tests were used. Spearman rank correlation coefficient (r) was used for correlation analysis. All statistical tests were two-sided, and significance was defined as $p < 0.05$. All statistical analysis was performed using SPSS, version 19, for Windows (SPSS, Chicago, IL).

3. Results

3.1. Time-course evolution of the ECG changes

Slope indices. An illustrative example of the evolution of QRS slopes during coronary occlusion is shown in figure 1(a). The displayed $\mathcal{I}_{\text{US}}$ and $\mathcal{I}_{\text{DS}}$ series correspond to precordial leads V1–V6 of a particular recording without any VT/VF episodes. That behavior is representative of most of the PCI recordings analyzed in the study.

For the case of the $\mathcal{I}_{\text{US}}$ index, the highest absolute changes were individually achieved between the 11th and 24th minute (related to the second remarkable peak shown in figure 1) after the start of occlusion. Mean ± SD and range for the timing of $\mathcal{I}_{\text{US}}$ peaks in the leads with the most changes (V2–V4) are summarized in table 2. In relation to this, two different incremental phases (two marked positive peaks) were found in $\mathcal{I}_{\text{US}}$ during the occlusion. The first peak was less prominent than the second one (see figure 1(a)). During the second half of the occlusion (approximately from minute 20), $\mathcal{I}_{\text{US}}$ normally started to decrease until the end of the recording, where it reached approximately the value observed before the occlusion started.

The time course of $\mathcal{I}_{\text{DS}}$ was substantially different to that of $\mathcal{I}_{\text{US}}$. The main difference was observed in the first half of the recording, where $\mathcal{I}_{\text{DS}}$ became lower in absolute value tending to zero (flatter slope) during the first 2 to 13 min of the occlusion. Then, $\mathcal{I}_{\text{DS}}$ started to decrease, achieving either a large negative peak or sometimes just a small negative deflection. The timing for the largest negative peak of $\mathcal{I}_{\text{DS}}$ ranged between the 7th and 20th minute after the start of occlusion. Mean ± SD and range for the timing of $\mathcal{I}_{\text{DS}}$ peaks are summarized in table 2.

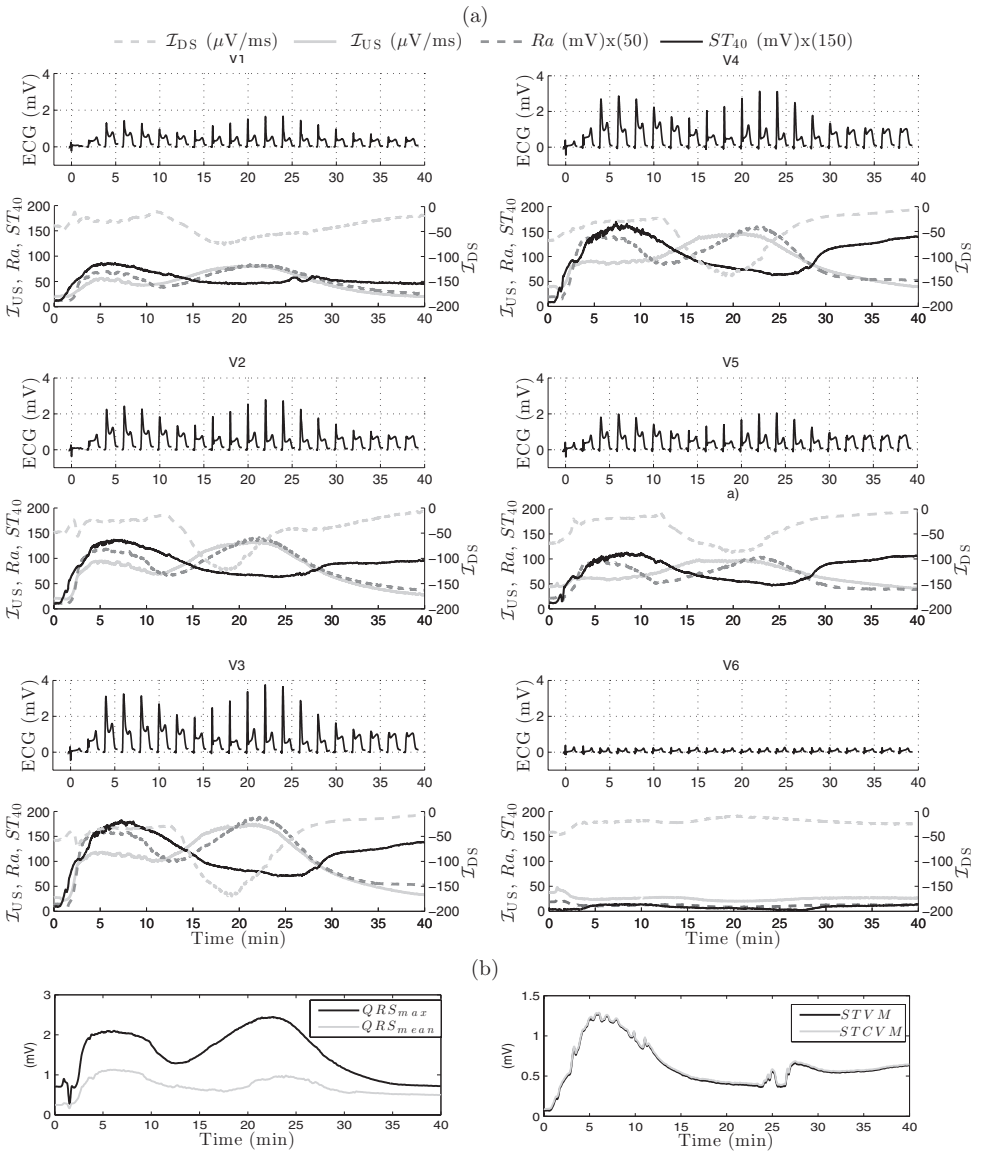

Figure 1. (a) Time course evolution of $\mathcal{I}_{US}$, R_a and ST_{40} (left axis), as well as $\mathcal{I}_{DS}$ (right axis), during 40 min occlusion for one particular recording, evaluated in precordial standard leads V1–V6. Odd rows display heartbeats recorded every 2 min in each precordial lead, and even rows present the series of the analyzed indices along the occlusion. (b) Time course evolution of indices derived from the VCG: QRS_{mean}, QRS_{max}, STVM and STCVM.

Regarding results obtained for the slopes evaluated in leads derived from the spatial QRS loop, mean $\pm$ SD of the timing corresponding to maximum (second positive peak) for $\mathcal{I}_{US}$ and both maximum (first positive peak) and minimum (second negative peak) for $\mathcal{I}_{DS}$ are also shown in table 2. In addition, figure 2 presents the time course of QRS slopes evaluated in the loop-derived lead for the same recording illustrated in figure 1. As can be observed from

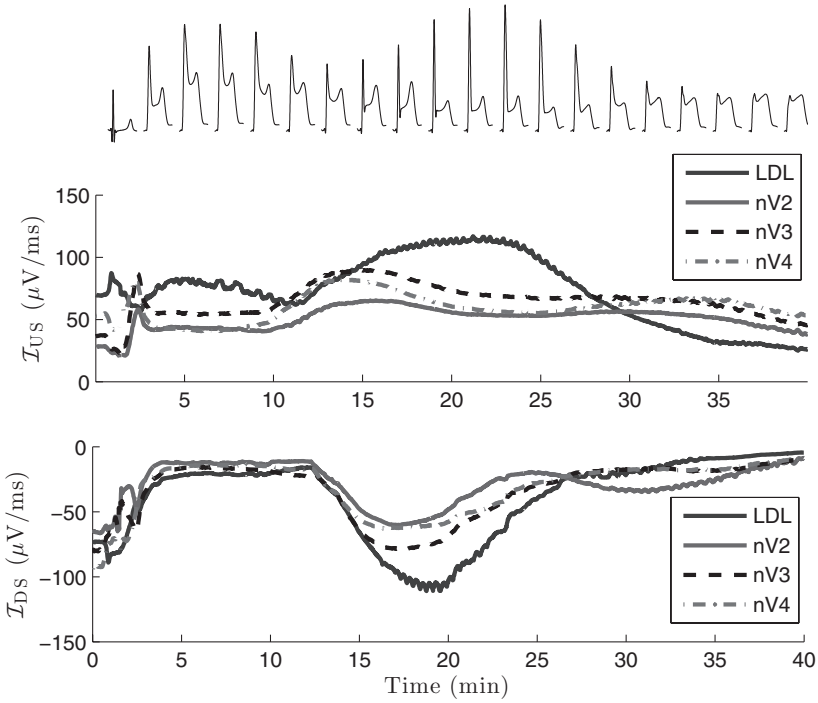

Figure 2. QRS slopes evaluated in the loop-derived lead (LDL) and in the normalized leads nV2–nV4 for the same pig as in figure 1. The top panel displays representative beats in the loop-derived lead every 2 min during the coronary occlusion.

Table 2. Average values and range for the timing of predominant peaks observed in $\mathcal{I}_{US}$ and $\mathcal{I}_{DS}$ in standard leads showing the largest changes (V2–V4) as well as in the lead derived from the QRS loop. LDL: loop-derived lead.

Lead	Timing of first peak Mean ± SD (range) (min) ($\mathcal{I}_{US}$)	Timing of second peak Mean ± SD (range) (min) ($\mathcal{I}_{US}$)	Timing of first peak Mean ± SD (range) (min) ($\mathcal{I}_{DS}$)	Timing of second peak Mean ± SD (range) (min) ($\mathcal{I}_{DS}$)
V2	4.6 ± 1.3 (2.3:6.7)	18.3 ± 2.4 (14.5:24.2)	4.9 ± 1.6 (3.5:7.7)	14.9 ± 4.0 (10.5:19.9)
V3	4.5 ± 1.5 (2.3:6.7)	18.2 ± 3.2 (14.7:23.5)	5.7 ± 2.7 (3.7:12.6)	14.5 ± 3.1 (10.4:19.8)
V4	–	16.3 ± 2.9 (11.3:19.9)	5.6 ± 3.1 (3.1:13.3)	14.7 ± 4.0 (7.1:19.7)
LDL	–	16.5 ± 2.5 (13.9:21.5)	4.7 ± 1.2 (3.0:7.5)	13.8 ± 4.0 (8.4:19.8)

figure 2, the first positive peak in $\mathcal{I}_{US}$ was found to be less pronounced than in precordial leads (illustrated in figure 1), while the second one was the most pronounced. In some cases, the first positive peak in $\mathcal{I}_{US}$ became negative, which is due to changes in the direction of the maximum magnitude vector within the QRS loop. In the case of $\mathcal{I}_{DS}$, the initial increase leading to the first positive peak was more relevant in the loop-derived lead, and then $\mathcal{I}_{DS}$ remained quite flat until the start of the negative deflection, keeping from that point on similar behavior to that observed in precordial leads.

The time course of QRS slopes evaluated in the normalized leads nV2–nV4 during coronary occlusion is displayed in figure 2. It can be observed that $\mathcal{I}_{DS}$ evaluated in these three precordial leads shows similar behavior to that observed in the loop-derived lead. Nevertheless, while in the original leads V2–V4 the evolution of $\mathcal{I}_{DS}$ is quite flat at the beginning of the occlusion, the normalized leads show a remarkable increase in $\mathcal{I}_{DS}$ during the first five minutes of occlusion. Subsequently, the $\mathcal{I}_{DS}$ index remains approximately constant for several minutes, which is followed by a large negative deflection. This behavior suggests that two important increases of QRS duration occur during the coronary occlusion in accordance with the two $\mathcal{I}_{DS}$ increases observed in the normalized leads. In contrast, the behavior of $\mathcal{I}_{US}$ in the normalized leads was quite different from that observed in the original leads (figure 1(a)) and in the loop-derived lead. In fact, only one clear positive peak was observed during the occlusion, which normally occurred in the time interval between the two positive peaks observed in the original leads. The observed differences in the evolution patterns of $\mathcal{I}_{US}$ and $\mathcal{I}_{DS}$ when analyzed in normalized and original ECG leads can be explained by the normalization process applied to the original leads, which separates the changes that occur in the slopes due to changes in the QRS duration and amplitude.

Conventional ECG indices. R-wave amplitude, R_a, and ST level deviation, ST_{40}, used here as conventional depolarization and repolarization indices, respectively, are shown in figure 1(a) for leads V1–V6. As can be observed from the figure, the R_a evolution during ischemia presents similar behavior to that observed for $\mathcal{I}_{US}$. In this case, a remarkable increase in R_a quickly developed at the start of occlusion, due to the fact that the rS complex configuration observed during the initial minutes turned into a monophasic, giant R wave. The initial R_a increase was transiently reduced until a second and more pronounced increase developed between the 11th and 24th minute. In the case of ST_{40}, a clear and unique positive peak was observed in most of the analyzed leads. This main peak in ST_{40}, indicating abrupt ST elevation, occurred between the 5th and 12th minute after the start of occlusion.

Vectorcardiogram-derived indices. In figure 1(b) four indices evaluated by using the VCG loop generated from orthogonal leads X, Y and Z are displayed. The left panel presents the QRS_{max} and QRS_{mean} series and the right panel, the STVM and STCVM series. A strong relationship was observed between the evolution of QRS_{max} calculated from the VCG and R_a evaluated in leads V1–V6, with two distinct phases clearly distinguished (see figure 1). A strong similarity was also found between STVM/STCVM and ST_{40}, with a predominant positive peak occurring during the first 10 min of occlusion.

3.2. Quantitative and dynamic ECG changes

The amount of changes induced by balloon inflation, as expressed by the parameter $\Delta\mathcal{Y}(t)$, was determined. Averaged values of delta change for all pigs, $\overline{\Delta\mathcal{Y}}(t)$, ($\mathcal{Y} \in \{\mathcal{I}_{US}, \mathcal{I}_{DS}, R_a, ST_{40}\}$) were computed in the precordial leads V1–V6. Similarly, $\overline{\Delta\mathcal{Y}}(t)$ values corresponding to those indices evaluated in leads derived from the QRS loop, $\mathcal{Y} \in \{\mathcal{I}_{US}, \mathcal{I}_{DS}\}$, and the VCG, $\mathcal{Y} \in \{QRS_{max}, QRS_{mean}, STVM, STCVM\}$, were also calculated.

The leads with the most substantial changes during occlusion were V2–V4 for the indices $\mathcal{I}_{US}$, $\mathcal{I}_{DS}$, R_a and ST_{40}. In figure 3 (top panels) averaged values, expressed as mean $\pm$ SD, for these four indices in lead V3 are shown. The first two panels at the top also display the averaged delta values for $\mathcal{I}_{US}$ and $\mathcal{I}_{DS}$ evaluated in normalized lead V3. Bottom panels of the same figure display the averaged delta values for $\mathcal{I}_{US}$ and $\mathcal{I}_{DS}$ evaluated in the loop-derived lead as well as QRS_{max} and STCVM indices evaluated

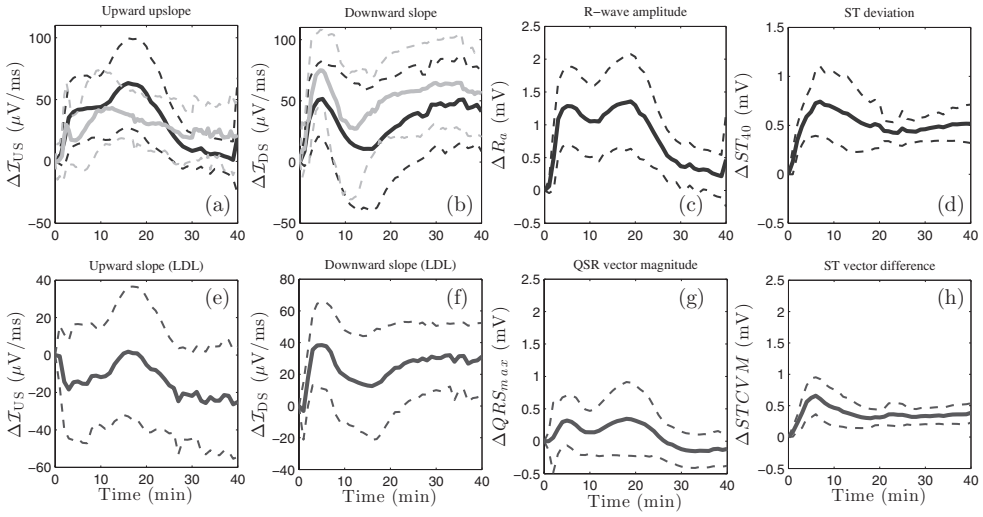

Figure 3. Top panels display mean ± SD of delta changes $\Delta\mathcal{Y}$, $\mathcal{Y} \in \{\mathcal{I}_{\mathrm{US}}, \mathcal{I}_{\mathrm{DS}}, R_a, \mathrm{ST}_{40}\}$ for all pigs in lead V3, calculated every minute from the start of occlusion: (a) $\mathcal{I}_{\mathrm{US}}$ in the original (black) and normalized lead V3 (gray); (b) $\mathcal{I}_{\mathrm{DS}}$ in the original (black) and normalized lead V3 (gray); (c) R_a; (d) ST_{40}. Bottom panels display mean ± SD of $\mathcal{Y}$, with $\mathcal{Y}$ being: (e) $\mathcal{I}_{\mathrm{US}}$ evaluated in QRS loop-derived lead; (f) $\mathcal{I}_{\mathrm{DS}}$ evaluated in QRS loop-derived lead; (g) $\mathrm{QRS}_{\mathrm{max}}$; (h) STCVM.

Table 3. Distribution of the largest changes across leads averaged over pigs for the different indices, expressed as mean ± SD. $\mathcal{I}_{\mathrm{US}}$ and $\mathcal{I}_{\mathrm{DS}}$ delta values are shown in both precordial and QRS loop-derived leads.

Lead	V2 Mean ± SD	V3 Mean ± SD	V4 Mean ± SD	LDL Mean ± SD	VCG Mean ± SD
$\Delta\mathcal{I}_{\mathrm{US}}$ (μV ms^{-1})	47.3 ± 32.2	63.4 ± 36.2	43.9 ± 39.6	1.79 ± 34.6	–
$\Delta\mathcal{I}_{\mathrm{DS}}$ (μV ms^{-1})	31.2 ± 25.5	51.6 ± 31.4	53.7 ± 36.4	38.4 ± 27.3	–
ΔR_a (mV)	1.04 ± 0.49	1.36 ± 0.72	0.96 ± 0.78	–	–
$\Delta\mathrm{ST}_{40}$ (mV)	0.59 ± 0.33	0.74 ± 0.36	0.57 ± 0.34	–	–
$\Delta\mathrm{QRS}_{\mathrm{max}}$ (mV)	–	–	–	–	0.36 ± 0.41
ΔSTCVM (mV)	–	–	–	–	0.66 ± 0.29

from the VCG. It is important to mention that, due to the presence of VT/VF episodes during occlusion, abnormal beats were discarded and it is thus possible that, at some time instants, not all pigs analyzed in this study are involved in the averages shown in figure 3. A summary of the most prominent changes found for all the indices shown in figure 3 is presented in table 3.

3.3. Correlation analysis between ECG changes and MaR

3.3.1. Correlation with MaR using absolute ECG changes during occlusion. Changes in the ECG indices during the occlusion were correlated with MaR defined in section 2.1.2. The overall mean ± SD and range of MaR in the study population was 39.0 ± 9.9 (range 28 to 57)% of the LV.

Table 4. Correlation values between MaR and $\Delta\mathcal{Y}$, $\mathcal{Y} \in \{\mathcal{I}_{US}, \mathcal{I}_{DS}, R_a, ST_{40}\}$, evaluated at the timings corresponding to the relevant peaks observed for each of those indices during the occlusion.

MaR versus $\Delta\mathcal{Y}$	$\Delta\mathcal{Y}_{max}$ $r(p)$	$\Delta\mathcal{Y}_{pos/neg}$ $r(p)$	$\Delta\mathcal{Y}_{abs}$ $r(p)$	$\Delta\mathcal{Y}_{real}$ $r(p)$
$\mathcal{I}_{US}$ First peak	0.54 (0.0850)	0.52 (0.0971)	0.69 (0.0167)	0.26 (0.4312)
$\mathcal{I}_{US}$ Second peak	0.42 (0.1929)	0.44 (0.1774)	0.41 (0.2092)	0.36 (0.2692)
R_a First peak	0.21 (0.5353)	0.43 (0.1825)	0.51 (0.1115)	0.44 (0.1724)
R_a Second peak	0.28 (0.4230)	0.34 (0.3025)	0.32 (0.3307)	0.20 (0.5628)
$\mathcal{I}_{DS}$ First peak	−0.75 (0.0045)	−0.65 (0.0220)	−0.63 (0.0265)	−0.66 (0.0184)
$\mathcal{I}_{DS}$ Second peak	−0.67 (0.0237)	−0.71 (0.0345)	−0.08 (0.8101)	−0.77 (0.0054)
ST_{40} peak	−0.25 (0.4351)	−0.34 (0.2814)	−0.34 (0.2805)	−0.34 (0.2828)

Upward slope change. Correlation analysis was performed considering $\Delta\mathcal{I}_{US}$ evaluated at the two prominent peaks identified during the occlusion in all the recordings. Results of the correlation analysis in the standard leads V1–V6 were not significant (N.S.) for the second prominent peak, while for the first one a significant correlation was found between $\Delta\mathcal{Y}_{abs}$ ($\mathcal{Y} = \mathcal{I}_{US}$) and MaR, $r = 0.69$ ($p = 0.0167$). Table 4 presents the correlation coefficients obtained for all combinations of change defined in subsection 2.5. Additionally, correlation analysis was performed for $\mathcal{I}_{US}$ evaluated in the loop-derived lead, and poor correlation values were obtained between MaR and the maximum positive change $\Delta\mathcal{Y}_{max}$ for the two peaks.

R-wave amplitude change. The R-wave amplitude changes, ΔR_a, in the two relevant peaks, were separately correlated with MaR. Correlation was, however, non-significant for any combination of change, as shown in table 4.

Downward slope change. As can be observed in table 4, there was a significant, negative correlation between this index and MaR. In the case of the first positive peak, these negative correlation values mean that more positive $\Delta\mathcal{I}_{DS}$ values ($\mathcal{I}_{DS}$ becoming less steep) correspond to smaller MaR. For the second negative deflection, these negative correlation values mean that lower $\Delta\mathcal{I}_{DS}$ values ($\mathcal{I}_{DS}$ becoming steeper) correspond to larger MaR. Regarding the first positive peak in the evolution of $\Delta\mathcal{I}_{DS}$ during occlusion, the most significant correlation was found between MaR and $\Delta\mathcal{Y}_{max}$, $r = -0.75$ ($p = 0.0045$), whereas for the second negative deflection in $\Delta\mathcal{I}_{DS}$, the most significant correlation was found between MaR and $\Delta\mathcal{Y}_{real}$, $r = -0.77$ ($p = 0.0054$). The delta value corresponding to the second negative deflection following the initial first positive peak takes either negative or positive value depending on the evaluated subject, and on average is close to zero, as can be appreciated in figure 4, which shows $\Delta\mathcal{I}_{DS}$ averaged over pigs every 10 s during occlusion in lead V3. The correlation results obtained for all combinations of change in $\Delta\mathcal{I}_{DS}$ are shown in table 4.

ST level change. The positive peak observed in ST_{40} during the first 10 min of occlusion is the most prominent one for this index. Similarly to the results obtained for $\Delta\mathcal{I}_{DS}$, correlation between ST_{40} and MaR was negative, although not significant, as summarized in table 4.

Figure 4 shows the time course evolution of $\Delta\mathcal{I}_{DS}$ averaged for all pigs and expressed as mean ± SD. Correlation values between MaR and the different combinations of change evaluated for $\Delta\mathcal{I}_{DS}$, but at the timings corresponding to the peaks found for each of the

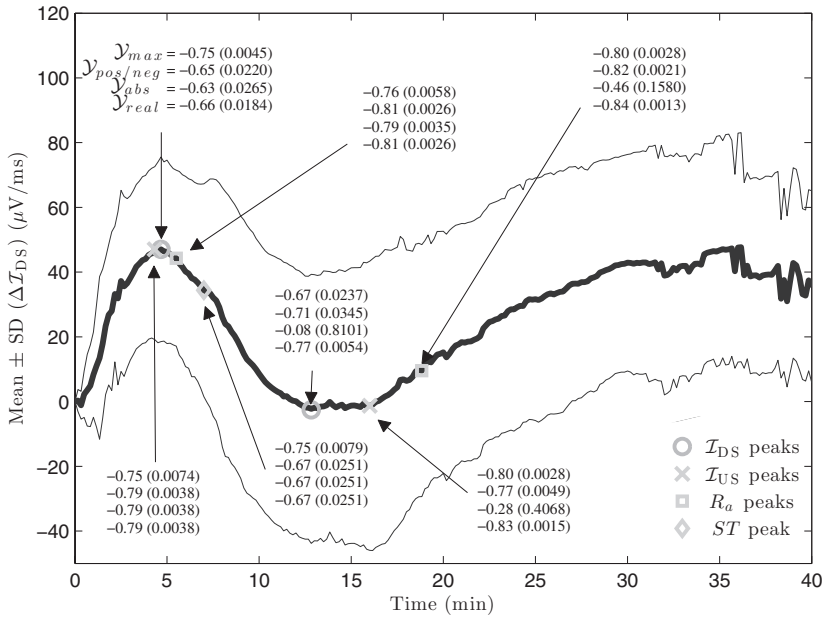

Figure 4. Average delta values of $\Delta\mathcal{I}_{DS}$ (mean ± SD) evaluated every 10 s from the start of occlusion. Gray marks (square, x-mark and diamond) indicate the timings of the relevant peaks found for each of the other indices, i.e. R_a, $\mathcal{I}_{US}$ and ST_{40}. The gray circles indicate the timing of $\Delta\mathcal{I}_{DS}$ positive peak and negative deflection. The numbers inside the graph express the correlation values obtained for $\mathcal{I}_{DS}$ combinations of change (ordered as in table 1) at specific time instants, which are pointed to their corresponding marks by black arrows.

other indices, are displayed in the figure in association with their positions in time. Increased correlation between $\Delta\mathcal{I}_{DS}$ and MaR was observed at some of those other temporal positions. Similarly to the results presented in figure 4 for$\Delta\mathcal{I}_{DS}$, correlation analysis was additionally performed for all the other indices, i.e. R_a, ST_{40} and $\Delta\mathcal{I}_{US}$, considering their delta changes evaluated at time instants associated with relevant peaks observed in the rest of the analyzed indices. Correlation values with MaR did not increase with respect to the results shown in table 4, except for $\Delta\mathcal{Y}_{max}$ for $\mathcal{Y} = \Delta\mathcal{I}_{US}$, evaluated at the timing of the positive peak corresponding to $\mathcal{I}_{DS}$, for which correlation with MaR was $r = 0.76$ ($p = 0.01$). Evaluation of the correlation between MaR and $\Delta\mathcal{I}_{US}$ and $\Delta\mathcal{I}_{DS}$ in normalized leads did not lead to higher correlation coefficients. For both indices, this correlation was non-significant in all cases. Evaluation of $\Delta\mathcal{I}_{US}$ and $\Delta\mathcal{I}_{DS}$ in normalized leads but considering the time instants corresponding to relevant peaks observed in the original leads did not increase the correlation values directly obtained for the original precordial leads.

Finally, correlation analysis carried out for QRS_{max}, QRS_{mean} and STCVM indices are summarized in table 5. None of these indices showed any significant correlation with MaR.

3.3.2. Correlation with MaR adding the temporal aspects of the peaks. The timings of relevant peaks in any lead and for any of the indices analyzed in this study did not correlate strongly with MaR. However, differences between the timings of the two more prominent peaks of R_a significantly correlated with MaR in lead V3, $r = -0.62$ ($p = 0.04$), indicating that shorter time between the two marked peaks was associated with larger MaR.

Indices combining absolute ECG changes occurring at prominent peaks with their corresponding timings, quantified by $\Delta\mathcal{Y}^l_{max} \cdot t^l_{max}$ and $\Delta\mathcal{Y}^l_{max}/t^l_{max}$, were also correlated with

Table 5. Correlation values between MaR and changes observed in STCVM, QRS_{max} and QRS_{mean}, at their most relevant peaks during occlusion.

Lead	$r(p)$
STCVM (max)	0.19 (0.5219)
QRS_{max} First peak	0.47 (0.1661)
QRS_{max} Second peak	0.42 (0.2202)
QRS_{mean} First peak	0.45 (0.1920)
QRS_{mean} Second peak	0.45 (0.1920)

MaR. In lead V3, both indices showed a negative correlation with MaR when $\Delta\mathcal{I}_{DS}$ was taken at the second negative peak ($r = -0.72$; $p = 0.01$ for $\Delta\mathcal{Y}^l_{max} \cdot t^l_{max}$ and $r = -0.68$; $p = 0.02$ for $\Delta\mathcal{Y}^l_{max}/t^l_{max}$. Likewise, the correlation was significant in lead V2, but just for $\Delta\mathcal{Y}^l_{max}/t^l_{max}$, with $r = -0.62$ ($p = 0.04$). In all other cases the correlation was N.S.

4. Discussion

Ischemia-induced ECG changes in depolarization and repolarization

In this study several indices derived from the ECG signal during both depolarization and repolarization phases were evaluated in an experimental, closed chest porcine myocardial infarction model produced by 40 min coronary balloon inflation.

Depolarization changes observed in R_a, $\mathcal{I}_{US}$ and QRS_{max} presented temporal patterns during the coronary occlusion that showed two well-defined phases, with two marked positive peaks. These two phases have been described for other electrophysiological indices and have been related to the incidence of arrhythmias (De Groot and Coronel 2004, Coronel *et al* 2002, Russell *et al* 1984, De Groot *et al* 2001). In the present study population, the largest changes of these QRS-derived indices, especially for $\mathcal{I}_{US}$ and QRS_{max}, were seen during the second phase rather than the first one, and were located in time between the 11th and 22nd minute of occlusion.

QRS_{max} and $\mathcal{I}_{US}$ are directly influenced by the R wave amplitude. As illustrated in figure 1, a giant R wave quickly developed during the first 4 min of coronary occlusion, and also later in time around 11–22 min. This particular finding has been reported in previous studies carried out in experiments with pigs (Chang *et al* 1989) and also in humans (Faillace *et al* 1985). However, those other studies did not focus their attention on the two different peaks in R_a evolution. Chang *et al* (1989) studied the presumable genesis for this giant R wave during transient transmural ischemia and hyperacute phase of transmural myocardial infarction by the analysis of different factors. They concluded that the origin of the giant R wave is the slowed conduction velocity into the ischemic tissue, which led to the formation of a homogeneous and discrete wavefront advancing toward the center of the ischemia from its lateral and subendocardial areas. These two local wavefronts do not cancel but instead complement each other. Thus, the activation of the ischemic tissue remains temporally isolated from the non-ischemic one giving rise to the development of a giant R wave. This appreciation was confirmed by Birnbaum and Drew (2003), who additionally mentioned that many other factors influence the R wave amplitude, so that this parameter is not helpful in determining the amount of developed myocardial ischemia, as corroborated in our study.

Somewhat different behavior was observed for the $\mathcal{I}_{DS}$ index, which presented a biphasic pattern, starting with a substantial decrease during the first 5 min (positive peak in $\Delta\mathcal{I}_{DS}$) followed by an increase until around the 12th minute, reflected in $\Delta\mathcal{I}_{DS}$ by a negative deflection. Subsequently, a second gradual decrease in $\mathcal{I}_{DS}$ was observed until the end of the occlusion

(figures 3(b) and (f)). That biphasic pattern was even more marked when $\mathcal{I}_{DS}$ was evaluated in normalized leads, suggesting an evident increase in the QRS width during the first minutes of occlusion, despite the fact that the QRS amplitude also increases during those first minutes. Figure 3(b) shows how the normalization procedure applied to the QRS amplitude emphasizes the first positive peak in $\Delta\mathcal{I}_{DS}$ of the normalized leads with respect to $\Delta\mathcal{I}_{DS}$ evaluated in the original precordial leads. Some minutes later during the occlusion and after the second negative deflection in $\Delta\mathcal{I}_{DS}$, $\mathcal{I}_{DS}$ became less steep again, even though QRS amplitude (see R_a and QRS_{max} indices in figures 3(c) and (g)) increased until around minute 20 and ST elevation became less marked. Finally, the further diminution of the R wave amplitude combined with the remaining ST elevation from minute 20 until the end of occlusion led to the continuous decline of the $\mathcal{I}_{DS}$ index.

ST-segment elevation, a classical index traditionally used for detecting transmural ischemia, developed a clear peak during the first 5–12 min of the occlusion in almost all the analyzed leads. After this time, the ST level started to decrease until the end of the occlusion, reaching around 50% of its maximal developed change (see figures 3(d) and (h)). The maximum peak of ST elevation at approximately 5–12 min as well as the latter decrease until the end of the coronary occlusion was similarly reported by Kjekshus *et al* (1972). Likewise, ST elevation was postulated as a valid marker of myocardial ischemia only in the first few minutes following the coronary occlusion, confirming that it became maximal around the initial 10–15 min with a subsequent decline after this time (Kleber *et al* 1978). As described earlier (Van Oosterom 1976), a plausible mechanism underlying the subsequent decline (after minutes 15–20) may be related to an increase of resistance between adjacent cells, affecting the gap junctions and leading to cell-to-cell uncoupling. This cell-to-cell uncoupling has been suggested to be triggered by a change in intracellular $[Ca^{2+}]$ (Noma and Tsuboi 1987, Firek and Weingart 1995, Dekker *et al* 1996).

Regarding the amount of change quantified by the parameter $\Delta\mathcal{Y}$ for all the analyzed indices, $\mathcal{Y} \in \{\mathcal{I}_{US}, \mathcal{I}_{DS}, R_a, ST_{40}\}$, it was found that lead V3 was the most sensitive, even more than leads derived from the spatial QRS loop, in contrast with our previous results in patients undergoing PCI (Romero *et al* 2011). This finding can be associated with the marked rotation observed in the maximum vector magnitude direction within the QRS loop, also reported in Näslund *et al* (1993a), which is used to project the VCG onto its dominant direction to obtain the QRS loop-derived lead. Care should be taken when interpreting changes just looking to electrophysiology and not realizing the geometrical implications.

Correlation between ECG changes and the amount of ischemia

In the correlation analysis the only parameters showing a significant correlation with MaR were the QRS slope changes. Of the classical ECG indices, neither ST elevation nor R_a showed any significant correlation with the amount of ischemia. However, in contrast to our previous findings in a human model of shorter transmural ischemia produced by PCI (Ringborn *et al* 2011), this longer, porcine experimental infarction model showed negative correlation between changes in the R-wave downslope, $\mathcal{I}_{DS}$, and MaR. This finding cannot be fully explained and further studies are needed to elucidate its underlaying basis.

Changes in the R-wave upslope, $\mathcal{I}_{US}$, showed a significant, however, positive correlation with MaR, as quantified using the sum of absolute change $\Delta\mathcal{Y}_{abs}$ in V1–V6 in the first peak, as well as the maximum change $\Delta\mathcal{Y}_{max}$ at the timing of the first, positive peak of $\mathcal{I}_{DS}$.

The correlation between MaR and QRS_{max}, which is a spatial projection of the maximum amplitude of the QRS complex, was also positive, a finding consistent with the results reported in [12], although in the present study it was non-significant.

As shown before, the QRS slope changes are dependent on both changes in the QRS amplitude and duration (Pueyo *et al* 2008). This is furthermore supported in this study by the results of the R-wave normalization, with loss of significance when correlating $\Delta\mathcal{I}_{DS}$ with MaR in the normalized leads, indicating that the combination of both QRS amplitude and duration variations reflected by $\Delta\mathcal{I}_{DS}$ better correlate with MaR than changes in $\mathcal{I}_{DS}$ due to the QRS width only. Additionally, it was shown that correlation was not significant between ΔR_a and MaR.

Another important finding of the present study was that all significant correlation values were found in standard precordial leads V1–V6. No extra value was added by using loop-derived leads, or vector-based QRS or ST indices.

Negative, non-significant correlation coefficients were obtained when ST_{40} changes were correlated with MaR, in agreement with the results reported by Demidova *et al* (2011) when investigating ST level changes in a subset of the present population. Many other studies, however, have shown opposite results when correlating ST level and MaR, both in humans and in animal experiments (Kjekshus *et al* 1972, Lowe *et al* 1978, Christian *et al* 1995). Our finding of negative correlation between MaR and ST_{40} cannot be clearly explained and needs to be further explored in future studies. One possible explanation could perhaps be that all subjects in the present study developed large anterior MaR (mean 39 ± 9.9, range 28 to 57% of the LV), and within this range and location the correlation between ECG indices and MPS might be different from the one evaluated for a wider range of ischemic areas including also much smaller areas as well as different locations of ischemia. However, this hypothesis needs to be confirmed in future studies.

Although the ST segment elevation during acute myocardial ischemia has been widely studied by many authors in both humans and animals, the relationship between alterations in depolarization and later signs of ischemic damage has been less studied. This study has shed light on that relationship.

Timing of ECG changes

One of the main observations of this study was that ST elevation peaked earlier in time than QRS_{max} and $\mathcal{I}_{US}$ (referring to the second peak of those two indices, of larger amplitude than the first one), indicating that more changes are still occurring during depolarization when changes at repolarization have already reached their maximum levels. Thus, changes in depolarization occurring some minutes later during occlusion could be in better correspondence with MaR as determined by MPS.

In relation to that, the correlation between $\mathcal{I}_{DS}$ and MaR was strong when the changes were evaluated at the most relevant peaks (positive and negative) observed in $\mathcal{I}_{DS}$, but even stronger for the second peak occurring later in time. Furthermore, the correlation between $\mathcal{I}_{DS}$ changes and MaR was not only significant when evaluated at its own peak values during the occlusion, but also when evaluated at the timing of the peaks of other indices, as displayed in figure 4. All the above arguments postulate the downward slope $\mathcal{I}_{DS}$, which combines both QRS amplitude and duration, as a potential predictor of the ischemic process.

5. Conclusions

In a porcine model of myocardial infarction, changes in the ECG related to the first half of the ventricular depolarization phase ($\mathcal{I}_{US}$, QSR_{max}) are mostly affected by the R-wave amplitude (R_a) variation, and do not strongly correlate with the myocardium at risk (MaR). However, indices related to the second part of the depolarization phase ($\mathcal{I}_{DS}$), which reflect changes

both in amplitude and width of the QRS complex, as well as distortion of the final part of the complex, are better predictors of the MaR in acute myocardial ischemia. The first 4–21 min of coronary occlusion represent the most significant ones in terms of correlation between changes in ECG-derived indices and the MaR.

Acknowledgments

This work was supported by projects TEC2010-21703-C03-02 and TEC2010-19410 from Spanish Ministry of Economy and Competitiveness (MINECO), Spain, and by the Donation funds at Skåne University Hospital, Lund, Sweden. EP acknowledges the financial support of Ramón y Cajal program from MINECO. MR acknowledges the Southern Healthcare Region, Lund, Sweden and Blekinge Scientific Council, Karlskrona, Sweden for financial support. Authors gratefully acknowledge valuable contribution of the imaging research group at the Department of Clinical Physiology and Nuclear Medicine, BFC, Skåne University Hospital in Lund (Sweden) for performing SPECT analyses on the experimental animals.

References

Abboud S, Cohen R J, Selwyn A, Ganz P, Sadeh D and Friedman P L 1987 Detection of transient myocardial ischemia by computer analysis of standard and signal-averaged high-frequency electrocardiograms in patients undergoing percutaneous transluminal coronary angioplasty *Circulation* **76** 585–96

Beker A, Pinchas A, Erel J and Abboud S 1996 Analysis of high frequency QRS potential during exercise testing in patients with coronary artery disease and in healthy subjects *Pacing Clin. Electrophysiol.* **19** 2040–50

Birnbaum Y and Drew B J 2003 The electrocardiogram in ST elevation acute myocardial infarction: correlation with coronary anatomy and prognosis *Postgrad. Med. J.* **79** 490–504

Birnbaum Y, Herz I, Sclarovsky S, Zlotikamien B, Chetrit A, Olmer L and Barbash G I 1996 Prognostic significance of the admission electrocardiogram in acute myocardial infarction *J. Am. Coll. Cardiol.* **27** 1128–32

Bolea J, Almeida R, Laguna P, Sörnmo L and Martínez J P 2009 BioSigBrowser, biosignal processing interface *ITAB 2009: 9th IEEE Int. Conf. on Information Technology and Applications in Biomedicine* pp 1–4

Chang W, Akiyama T, Richeson J, Faillace R and Serrino P 1989 Origin of the giant R wave in acute transmural myocardial infarction in the pig *Japan. Heart J.* **30** 863–83

Charlap S, Shani J, Schulho N, Herman B and Lichstein E 1990 R- and S-wave amplitude changes with acute anterior transmural myocardial ischaemia *Chest* **97** 566–71

Christian T, Gibbons R, Clements I, Berger P, Selvester R and Wagner G 1995 Estimates of myocardium at risk and collateral flow in acute myocardial infarction using electrocardiographic indexes with comparison to radionuclide and angiographic measures *J. Am. Coll. Cardiol.* **26** 388–93

Coronel R, Wilms-Schopman F and De Groot J 2002 Origin of ischemia-induced phase 1b ventricular arrhythmias in pig hearts *J. Am. Coll. Cardiol.* **39** 166–76

De Groot J and Coronel R 2004 Acute ischemia-induced gap junctional uncoupling and arrhythmogenesis *Cardiovasc. Res.* **62** 323–34

De Groot J, Wilms-Schopman F, Opthof T, Remme C and Coronel R 2001 Late ventricular arrhythmias during acute regional ischemia in the isolated blood perfused pig heart. Role of electrical cellular coupling *Cardiovasc. Res.* **50** 362–72

Dekker L, Fiolet J, Van Bavel E, Coronel R, Opthof T, Spaan J and Janse M J 1996 Intracellular Ca^{2+}, intercellular electrical coupling, and mechanical activity in ischemic rabbit papillary muscle. Effects of preconditioning and metabolic blockade *Circ. Res.* **79** 237–46

Demidova M, van der Pals J, Ubachs J, Kanski M, Engblom H, Erlinge D, Tichonenko V and Platonov P 2011 ST-segment dynamics during reperfusion period and the size of myocardial injury in experimental myocardial infarction *J. Electrocardiol.* **44** 74–81

Edenbrandt L and Pahlm O 1988 Vectorcardiogram synthesized from a 12-lead ECG: superiority of the inverse Dower matrix *J. Electrocardiol.* **21** 361–7

Faillace R, Akiyama T and Chang W 1985 The giant R wave of acute myocardial infarction *Japan. Heart J.* **26** 165–78

Firek L and Weingart R 1995 Modification of gap junction conductance by divalent cations and protons in neonatal rat heart cells *J. Mol. Cell. Cardiol.* **27** 1633–43

Heiberg E, Sjögren J, Ugander M, Carlsson M, Engblom H and Arheden H 2010 Design and validation of segment-freely available software for cardiovascular image analysis *BMC Med. Imaging* **10** 1

Janse M J, Cinca J, Morena H, Fiolet J W, Kleber A G, de Vries G P, Becker A E and Durrer D 1979 The border zone in myocardial ischemia. An electrophysiological, metabolic, and histochemical correlation in the pig heart *Circ. Res.* **44** 576–88

Kjekshus J, Maroko P and Sobel B 1972 Distribution of myocardial injury and its relation to epicardial ST-segment changes after coronary artery occlusion in the dog *Cardiovasc. Res.* **6** 490–9

Kleber A, Janse M, Van Capelle F and Durrer D 1978 Mechanism and time course of ST and TQ segment changes during acute regional myocardial ischemia in the pig heart determined by extracellular and intracellular recordings *Circ. Res.* **42** 603–13

Lowe J E, Reimer K A and Jennings R B 1978 Experimental infarct size as a function of the amount of myocardium at risk *Am. J. Pathol.* **90** 363–79 PMID: PMC2018154

Martínez J P, Almeida R, Olmos S, Rocha A P and Laguna P 2004 A wavelet-based ECG delineator: evaluation on standard databases *IEEE Trans. Biomed. Eng.* **51** 570–81

Morena H, Janse M J, Fiolet J W, Krieger W J, Crijns H and Durrer D 1980 Comparison of the effects of regional ischemia, hypoxia, hyperkalemia, and acidosis on intracellular and extracellular potentials and metabolism in the isolated porcine heart *Circ. Res.* **46** 634–46

Näslund U, Häggmark S, Johansson G and Reiz S 1993a Ischaemia and reperfusion induced transient QRS vector changes: relationship to size of the ischaemic territory *Cardiovasc. Res.* **27** 327–33

Näslund U, Häggmark S, Johansson G and Reiz S 1993b Quantification of myocardium at risk and detection of reperfusion by dynamic vectorcardiographic ST segment monitoring in a pig occlusion–reperfusion model *Cardiovasc. Res.* **27** 2170–8

Noma A and Tsuboi N 1987 Dependence of junctional conductance on proton, calcium and magnesium ions in cardiac paired cells of guinea-pig *J. Physiol.* **382** 193–211 (available at http://jp.physoc.org/content/382/1/193.short)

Pettersson J, Pahlm O, Carro E, Edenbrandt L, Ringborn M, Sörnmo L, Warren S G and Wagner G S 2000 Changes in high-frequency QRS components are more sensitive than ST-segment deviation for detecting acute coronary artery occlusion *J. Am. Coll. Cardiol.* **36** 1827–34

Pueyo E, Sörnmo L and Laguna P 2008 QRS slopes for detection and characterization of myocardial ischemia *IEEE Trans. Biomed. Eng.* **55** 468–77

Ringborn M, Romero D, Pueyo E, Pahlm O, Wagner G S, Laguna P and Platonov P 2011 Evaluation of depolarization changes during acute myocardial ischemia by analysis of QRS slopes *J. Electrocardiol.* **44** 416–24

Romero D, Ringborn M, Laguna P, Pahlm O and Pueyo E 2011 Depolarization changes during acute myocardial ischemia by evaluation of QRS slopes: standard lead and vectorial approach *IEEE Trans. Biomed. Eng.* **58** 110–20

Russell D, Lawrie J, Riemersma R and Oliver M 1984 Mechanisms of phase 1a and 1b early ventricular arrhythmias during acute myocardial ischemia in the dog *Am. J. Cardiol.* **53** 307–12

Weston P, Johanson P, Schwartz L M, Maynard C, Jennings R B and Wagner G S 2007 The value of both ST-segment and QRS complex changes during acute coronary occlusion for prediction of reperfusion-induced myocardial salvage in a canine model *J. Electrocardiol.* **40** 18–25

Van Oosterom A 1978 Cardiac potential distributions *PhD Dissertation* University of Amsterdam, The Netherlands